

Performance of the PAMELA space telescope in the identification of the light nuclei cosmic rays component

Valeria Malvezzi¹ for the PAMELA Collaboration

Abstract—PAMELA is a space telescope orbiting around the Earth since the 15th of June 2006. The orbit is elliptical and semi-polar, with an inclination of 70° and an altitude varying between 350 km and 610 km. The scientific objectives addressed by the mission are the measurement of the antiprotons and positrons spectra in cosmic rays, the hunt for anti-nuclei as well as the determination of light nuclei fluxes from hydrogen to oxygen in a wide energy range and with high statistics. Accurate measurements of the elemental composition of cosmic rays over a wide energy range are required in order to understand the origin, propagation and lifetime of the cosmic radiation. The primary cosmic rays (e.g. C, N and O), produced at the sources, propagate through the interstellar medium giving information about the composition at the source. Secondary elements (e.g. Li, Be, and B) are tracers of amount of matter traversed by the cosmic rays. PAMELA will measure the light nuclear component of Galactic cosmic rays in the interval 100 MeV/n-150 GeV/n with an accuracy overcoming the uncertainties of the current propagation models. The analysis techniques shown in this proceeding demonstrate that spectrometer, time-of-flight system (ToF) and calorimeter are able to discriminate light-charged particles.

I. INTRODUCTION

Cosmic rays (CRs) were discovered by Victor Hess in 1912. Today their origin is still unclear. CRs have been studied in experiments above the atmosphere, in the atmosphere, on the ground, underground and in space. Their energies cover an enormous range, from sub GeV to more than a few 10^{11} GeV, over which their differential flux decreases by roughly 33 orders of magnitude (figure 1). This flux can be approximated by a broken power-law, $dn/dE \sim E^{-\delta}$, with a series of breaks near 3 PeV known as the knee, a second knee near 200 PeV and an ankle near 4 EeV. The power-law index changes from $\delta \approx 2.67$ below the knee to $\delta \approx 3.05$ above it and steepens to $\delta \approx 3.2$ at the second knee [2] [3]. At the ankle, the spectral index changes to $\delta \approx 2.7$.

The cosmic rays in the energy range from several GeV up to about 100 PeV are assumed to be mostly of galactic origin, while at energies between the knee and the ankle their galactic or extragalactic origin is not yet clarified [4]. CRs with energy above the ankle are generally believed to be extragalactic in origin because they can no longer be isotropized by the Galactic magnetic fields while their arrival directions are isotropic to a fair approximation. At energies up to around the knee the CRs energy spectra can be measured

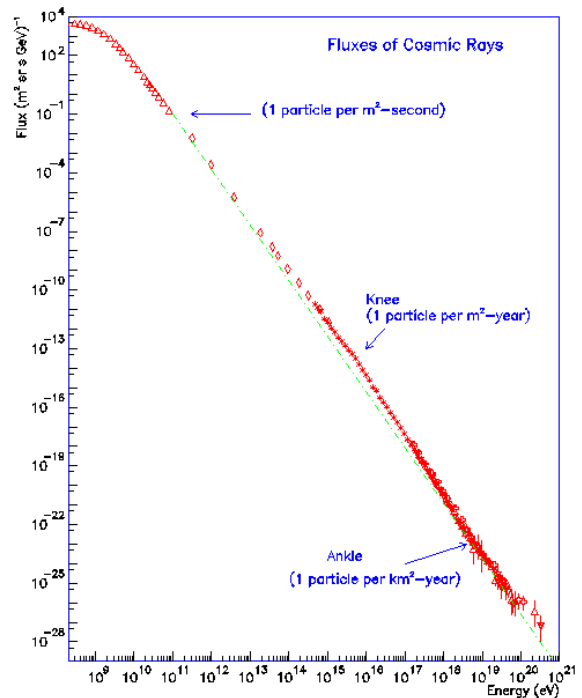


Fig. 1. All particle cosmic rays energy spectrum [1].

in a direct way with experiments on balloons at the top of the atmosphere or in space on board satellites or outside the ISS. At energies above 1 PeV the steeply falling spectrum requires large detection areas and exposure times of several years [5], so that only on ground indirect measurements are available.

The understanding of the origin of the Galactic Cosmic Rays (GCRs) is an old and refractory problem. There are actually several distinct questions. The first concerns the origin of the energy. What powers the accelerator and how does it work? The second regards the source of the particles which are accelerated. Out of what component of the Galaxy does the accelerator select particles to turn into cosmic rays? Third, there is the question of how much of the observed cosmic ray spectrum is in fact of Galactic origin. Over what energy range does the accelerator work and what spectral form does its output have? Finally, there is the question of how many different types of accelerator are required. Can one basic process explain all the data, or do we need to invoke multiple sources and mechanisms? Of course a satisfactory physical

¹INFN Sezione di Roma Tor Vergata, Via della Ricerca Scientifica 1, Rome, Italy, I-00133, valeria.malvezzi@roma2.infn.it, <http://pamela.roma2.infn.it>

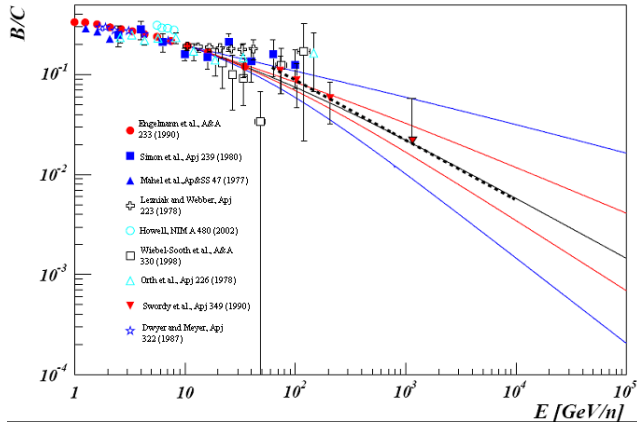


Fig. 2. B/C ratio as a function of kinetic energy per nucleon. Solid curves correspond to theoretical predictions [10]; dashed line is a simple power law spectrum $B/C = 1.4E^{-0.60}$.

model for the origin of the GCRs should simultaneously answer all these questions [6].

A theory on particles acceleration which is sufficiently well developed to allow quantitative model calculations, and which appears capable of meeting many of the observational constraints on any cosmic ray acceleration theory, is the diffusive acceleration applied to the strong shocks associated with supernova remnants (SNRs) [7] [8].

After acceleration, the particles propagate in a diffusive process through the Galaxy, being deflected many times by the randomly oriented magnetic fields ($B \sim 3 \mu G$). The nuclei are not confined to the galactic disc, they propagate in the galactic halo as well. The diffuse γ -ray background, extending well above the disc, detected by the EGRET experiment, exhibits a structure in the GeV region, which is interpreted as indication for the interaction of propagating CRs with interstellar matter [9]. The measured abundance of radioactive nuclei in CRs yields a residence time in the Galaxy of about 15×10^6 yr, for particles with GeV energies. Information on the propagation pathlength of CRs is often derived from the measurement of the ratio of primary to secondary nuclei. The first are produced through spallation during propagation in the Galaxy. As an example, the measured boron-to-carbon ratio is shown in figure 2 as function of energy [10]. The energy dependence of the measured ratio is frequently explained in Leaky Box models by a decrease of the pathlength of CRs in the Galaxy.

Ratios such as D/p , ${}^3He/{}^4He$ and B/C give information on the interstellar medium since all compare the abundances of secondary and primary species. The beryllium isotope ratio ${}^{10}Be/{}^9Be$ is a probe for galactic confinement times since both isotopes are secondary but one of them, ${}^{10}Be$, is unstable ($t_{1/2} = 1.5 \times 10^6$ yr). The composition of low energy cosmic rays provides important hints to the acceleration processes and the propagation of cosmic rays through the interstellar medium (ISM). Especially important in this respect are the abundances and spectra of elements such as Boron, Beryllium and Lithium, which are mainly produced as secondaries of primary cosmic

rays. The ratio of secondary to primary (for instance B/C) cosmic ray fluxes provides a unique tool to characterize the diffusion properties of the ISM [11].

To clarify the role of the different mechanisms that act in the propagation of Galactic cosmic rays it is fundamental to have more precise and extended data on the secondary/primary abundance ratios (like the ratio B/C) and on the fluxes of primary particles: in this field PAMELA can represent a big step ahead. Object of this paper is the presentation of the light-charge identification capabilities of PAMELA, as evaluated during the first two years of flight.

II. THE PAMELA SPACE MISSION

PAMELA – *Payload for Matter-Antimatter Exploration and Light Nuclei Astrophysics* – is an international collaboration constituted by several INFN and Italian Universities, three Russian institutions (MEPhI and FIAN Lebedev in Moscow and IOFFE in St. Petersburg), the University of Siegen in Germany and the Royal Technical Institute in Stockholm, Sweden. The PAMELA mission focuses on the investigation of dark matter, cosmic ray generation and propagation in our galaxy and the solar system, and studies of solar modulation and the interaction of cosmic rays with the Earth’s magnetosphere. The primary scientific goal is the study of the antimatter component of the cosmic radiation, with the following themes in mind:

- To search for evidence of dark matter particle annihilations by precisely measuring the antiparticle (antiproton and positron) energy spectra.
- To search for primordial antinuclei (e.g. antihelium) and evidence for antistellar nucleosynthesis (e.g. anticarbon)
- To test cosmic-ray propagation models through precise measurements of the antiparticle energy spectrum and precision studies of light nuclei and their isotopes.

Table I shows the nominal design goals for PAMELA performance, the various cosmic-ray components energy ranges over which PAMELA will provide new results are indicated.

	Energy range
Antiproton flux	80 MeV - 150 GeV
Positron flux	50 MeV - 300 GeV
Electron/positron flux	up to 2 TeV (from calorimeter only)
Electron flux	up to 500 GeV
Proton flux	up to 700 GeV
Light nuclei (up to Z=6)	up to 200 GeV/n
Antinuclei search	sensitivity of $O(3 \times 10^{-8})$ for He-bar/He

TABLE I
PAMELA DESIGN PERFORMANCE

In figures 3(a) and 3(b) the arrangement of the PAMELA apparatus and the Flight Model are shown.

The core of the apparatus is a magnetic spectrometer, composed of a permanent magnet, with an almost uniform magnetic field of 0.43 T, and of a tracking system made up of six equidistant silicon detector planes composed of two double sided microstrip layers, 300 μm thick each [12]. The resolution in the bending side is 4 μm and the MDR is 800

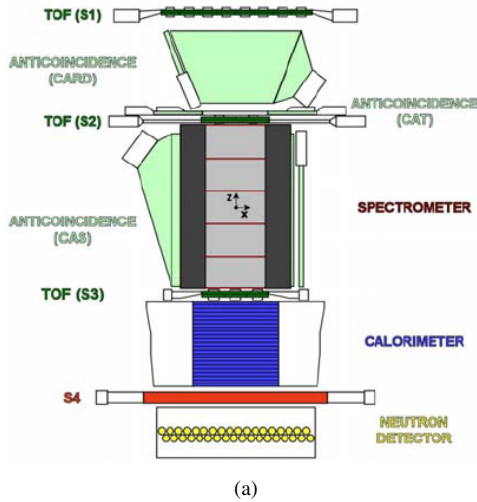


Fig. 3. Scheme of PAMELA instrument (a) and photo of PAMELA Flight Model(b).

GV.

The separation between the leptonic and hadronic components is assured by two detectors, an imaging calorimeter [13] and a neutron detector [14]. The calorimeter is composed by 44 ministrip silicon layers, $380 \mu\text{m}$ thick each, interleaved with 22 tungsten planes for a depth of 16 radiation lengths and 0.6 interaction lengths.

A large thick scintillator (S4) and a neutron detector located below the calorimeter give a supplementary tool in the discrimination between hadron/lepton [15]. In fact, a shower induced in the calorimeter by an hadron contains many more neutrons than a shower produced by an electron.

A set of 3 pairs of stripped plastic scintillators constitutes the PAMELA trigger and Time-of-Flight [16]. An additional set of plastic scintillators in anticoincidence defines the acceptance of the particles inside the spectrometer [17]. The geometry factor of the instrument is $21.5 \text{ cm}^2\text{sr}$ and the total weight is 470 Kg. A complete description of the subdetector components can be found in [18].

III. CHARGE IDENTIFICATION AND INTRINSIC DETECTORS RESOLUTION

PAMELA can determine the particle charge in a redundant way, by means of the Time-of-Flight scintillating paddles, the silicon microstrips of the tracking system and the ministrips of the imaging calorimeter. In this section the intrinsic detector resolutions in Z reconstruction will be presented.

A. Nuclei Identification with ToF

The time-of-flight system provides the charge of the incident particles by the energy deposit (dE/dx) measurements in the scintillators and the determination of particles velocity up to energies of about 3 GeV/nucleon. The particle velocity, β , is determined by measuring the flight time between two scintillators planes of the ToF. In this way, we have more than one β evaluation. Once β has been determined, the dE/dx , in

any of the ToF layers, will vary as a function of both velocity and charge as shown in figure 4 for the plane S31. The energy

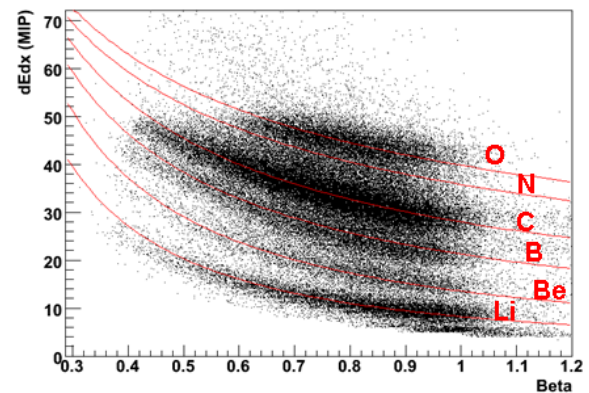


Fig. 4. Plot of energy loss (dE/dx) in the scintillator S31 vs. particle velocity. Superposed are the derived charge-band fits.

loss presented in the figure is corrected for the incident angle of the particle and light attenuation within the scintillator.

The measured particles clearly fall into distinct, easily identified charge bands. Such bands can be fitted, as shown by the curves superimposed to the points. A charge scale for each scintillator was derived from the results of these fits [19]. The six scintillator layers enable six independent charge determinations, thus significantly improving the charge resolution of the whole ToF system. Combining by a weighed average the charges reconstructed with this method, the charge resolution presented in figure 5 is reached. The charge peaks have been fitted by a Gaussian curve with the following peak/sigma: 3.00/0.11; 4.00/0.14; 4.99/0.18; 5.99/0.21.

B. Nuclei Identification with Tracker

The tracking system can be used to determine the absolute value of the charge by multiple measurements of the mean rate of energy loss in the silicon sensor and by the magnetic

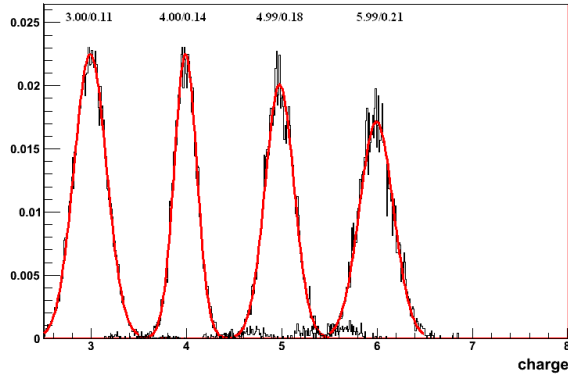


Fig. 5. Charge separation in ToF system; the histograms are normalized to the number of events. The gaussian fit of the peak gives the detector charge resolution.

rigidity, $R = p/Ze$ (where p = particle momentum, Z =particle charge). Using the same technique described above for the ToF system, a charge scale from the fit of dE/dx vs. rigidity was obtained. Selecting a clean sample of nuclei from $Z=3$ up to $Z=6$, we obtain the charge resolution presented in figure 6, where histograms are normalized to the number of events. In this way no interaction or conversion happened to the particle through the detector. Fitting the peaks with a Gaussian curve we have obtained the following peak/sigma: 2.99/0.16; 4.00/0.23; 4.98/0.28; 6.01/0.34.

C. Nuclei Identification with Calorimeter

The dE/dx measurement on the calorimeter silicon planes can be used to determine the charge of the incident nuclei too. The particle charge can be measured in the calorimeter by considering the energy released in one or more than one plane of the detector. Obviously, charge separation increases with the number of planes required but the efficiency of the measurement decreases. With this detector, as well, is possible to reconstruct a charge scale from the fit of dE/dx vs. β or R , depending on the energy range we are investigating. In figure 7 the charge resolution obtained considering only the first plane and the particle velocity, β , is shown; the histogram is normalized to the number of events and cuts are applied to be sure that no interaction occurred in the detectors above the calorimeter. In this case the Gaussian fit of the

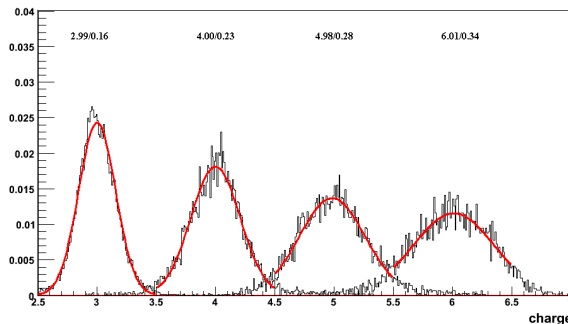


Fig. 6. Spectrometer charge resolution normalized to the number of events.

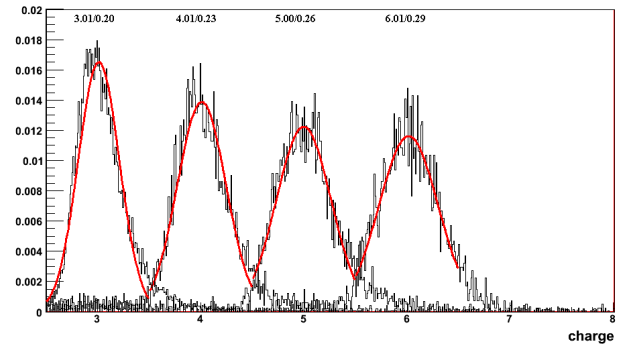


Fig. 7. Calorimeter charge resolution normalized to the number of events.

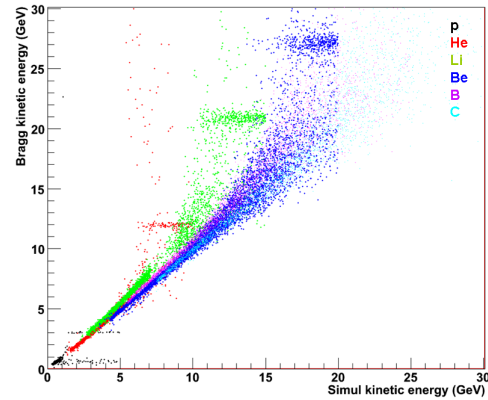


Fig. 8. Reconstructed kinetic energy vs. simulated one for events with right charge identification with the Bragg technique.

peaks gives the following peak/sigma: 3.01/0.20; 4.01/0.23; 5.00/0.26; 6.01/0.29.

Such a sampling calorimeter allows another method to identify the charge and the energy of the particle. For non-interacting events with energy below 2 GeV/n, an iterative algorithm to reconstruct Z and E has been developed. All the energy losses in the planes preceding the Bragg peak are fitted with a Bethe-Bloch curve with Z , A and E as free parameters. The efficiency of this method has been studied with simulated data; figure 8 shows the reconstructed energy vs simulated one for events with right charge identification.

IV. CONCLUSION

In this paper preliminary results on PAMELA charge identification capabilities and the consequent charge resolution has been presented. The numbers reported show that the tracking system, optimized for $Z=1$ particles, can contribute with a good charge resolution at least up to Lithium (when the single-channel saturation of the silicon sensors reduces the performances). The calorimeter has instead good charge resolution at least up to $Z=8$. The ToF seems to be the most powerful detector; it can evaluate the particle charge also in the cases in which the tracking algorithm was not able to reconstruct a track, and the elemental separation is better than in the other two detectors for nuclei with Z more than 3. With these performances PAMELA confirms the possibility

to improve our knowledge in the mechanisms involved in the generation, acceleration and propagation of cosmic rays.

REFERENCES

- [1] Bhattacharjee, P. and Sigl, G., *Origin and Propagation of Extremely High Energy Cosmic Rays*, Phys. Rept. 327, 109, 2000.
- [2] Olinto, A.V., *Highest Energy Cosmic Rays*, ArXiv e-print: 0410685, astro-ph, 2004.
- [3] Cronin, J.W., *The highest-energy cosmic rays*, ArXiv e-print: 0402487v1, astro-ph, 2004.
- [4] Allard, D., Parizot, E. and Olinto, A.V., *On the transition from Galactic to extragalactic cosmic-rays: spectral and composition features from two opposite scenarios*, Astropart. Phys., 27, 61-75, 2007.
- [5] Hörandel, J.R., *Overview on direct and indirect measurements of cosmic rays*, ArXiv e-print: 0501251v1, astro-ph, 2005.
- [6] Drury, L. O.C., Ellison, D. C., et al., *Tests of Galactic Cosmic Ray Source Models*, ArXiv e-print: 0106046v1, astro-ph, 2001.
- [7] L.G. Sveshnikova et al., *The knee in galactic cosmic ray spectrum and variety in supernovae*, A& A, 409, 799, 2003.
- [8] K. Kobayakawa et al., *Acceleration by oblique shocks at supernova remnants and cosmic ray spectra around the knee region*, Phys. Rev. D 66, 083004, 2002.
- [9] A.W. Strong & I.V. Moskalenko, *Galactic cosmic rays & gamma rays: a synthesis*, Proc. Workshop "LiBeB, Cosmic Rays and Gamma-Ray Line Astronomy", eds. R. Ramaty, E. Vangioni-Flam, M. Casse, and K. Olive, ASP Conf. Ser., v.171, pp.162-169, 1999.
- [10] A. Castellina, and F. Donato, *Diffusion coefficient and acceleration spectrum from direct measurements of charged cosmic ray nuclei*, Astropart. Phys., 24, 146-159, 2005.
- [11] D. Maurin et al., *Galactic Cosmic Ray Nuclei as a tool for Astroparticle Physics*, ArXiv e-print: 0212111, astro-ph, 2002.
- [12] O. Adriani et al., *The magnetic spectrometer of the PAMELA satellite experiment*, Nucl. Instr. and Meth. A, 511, 72, 2003.
- [13] M. Boezio et al., *The electronhadron separation performance of the PAMELA electromagnetic calorimeter*, Astrop. Phys., 26, 111, 2006.
- [14] A.M. Galper, *Measurement of primary protons and electrons in the energy range of $10^{11} - 10^{13}$ eV in the PAMELA experiment*, Proceeding of ICRC, 2219, 2001.
- [15] V. Malvezzi et al., *Performance of neutron detector and bottom trigger scintillator of the space instrument PAMELA*, Proc 9th ICATPP Conference, Como, 957, 2005.
- [16] G. Osteria et al., *The time-of-flight system of the PAMELA experiment on satellite*, Nucl. Instr. and Meth. A, 535, 152, 2004.
- [17] S. Orsi et al., *Pre-Flight Performance Studies of the Anticoincidence Systems of the PAMELA Satellite Experiment*, Proc. 29th International Cosmic Ray Conference, Pune, vol. 3, 369, 2005.
- [18] Picozza, P., et al., *PAMELA A payload for antimatter matter exploration and light-nuclei astrophysics*, Astropart. Phys., 27, 296, 2007.
- [19] T. Hams, et al., *Measurements of the abundance of radioactive ^{10}Be and other Light Isotopes in Cosmic Radiation up to 2 GeV nucleon $^{-1}$ with the Balloon-Borne instrument ISOMAX*, ApJ, 611, 892-905, 2004.